Proceedings of Ninth World Conference on Earthquake Engineering
August 2-9, 1988, Tokyo-Kyoto, JAPAN (Vol.VIII)

SF-7

ELASTIC-PLASTIC EARTHQUAKE RESPONSE ANALYSIS OF REINFORCED CONCRETE FRAME IN CONSIDERATION OF FLUCTUATION OF AXIAL FORCES ON COLUMNS

Eiji FUKUZAWA[1], Yutaka ISOZAKI[1] and Kouji FUJISAKI[2]

[1]Architectural Design Division, Kajima Corporation,
[2]Shinjuku-ku, Tokyo, Japan
[2]Information System Center, Kajima Corporation,
Minato-ku, Tokyo, Japan

SUMMARY

This paper presents the rigorous elastic-plastic earthquake response analytical method which was newly developed in considering the fluctuation of axial forces on columns for the highrise reinforced concrete(RC) frame. By using this method, both the simulation analysis of the structural tests of columns with core rebars and the earthquake response analysis of a 30 story RC frame against hypothetically worst earthquakes are conducted in order to verify this method and to investigate its inelastic response behavior under the fluctuating axial forces of columns.

INTRODUCTION

On the columns of the highrise RC frame, their elastic-plastic properties such as instantaneous rigidities, crack stresses and yield stresses are varied from moment to moment by the fluctuating axial forces during earthquake. For example, on the exterior columns, at the tension side crackings occur earlier and their rigidities and strengths decrease, while at the compression side crackings occur later and their rigidities decrease little. Therefore, as an object of the RC framing structure two surfaces of crack and yield are introduced on the force plane of bending moment(M) and axial force(N) at the ends of column. And by extending the degrading tri-linear bystresis loops proposed by Dr. Muto(Ref.1) to the M-N force plane for the earthquake repeated loads, the elastic-plastic earthquake response analytical method is newly developed.

ANALYTICAL METHOD

Basic Assumption

1) In the RC frame composed of columns, beams and joint panels, their elastic-plastic properties are considered in the bending and axial deformations of columns and the bending deformations of beams. The shearing deformations of members are assumed to maintain elastic.

2) Regarding columns, as shown in Fig.1, two surfaces of crack and yield are introduced on the M-N force plane at the ends of columns as the yield criteria. The yield surface is assumed as parabolic curves approximated from M-N values at the ultimate strengths which are obtained by summation of M-N strength curves of concrete and reinforcing bars. The crack surface is assumed as similar parabolic curves to the yield one and to have the same center as the yield one has.

3) Three states of elastic, crack and yield are assumed at column ends. In the elastic state, the stress point, nP(M, N) is located within the crack surface. In the crack state, the stress point is located on the crack surface which expands maintaining as the similar shape to the yield one. In the yield state, the crack surface is identified to the yield one. The stress point is located on the yield surface which expands and transfers.
4) The uniaxial M-θ (θ : tangential bending rotation angle at the column end) hysteresis loop is assumed the degrading property of the trilinear type, as shown in Fig.2, against the repeated anti-symmetric distributed moment under the constant axial force No (No: axial force value at the center of the initial yield and crack surfaces.)
5) The uniaxial N-ω (ω : relative axial deflection between top and bottom of column) hysteresis loop is assumed the degrading trilinear property, as shown in Fig.3, against the repeated axial force under the condition where M is zero.
6) Regarding beams, the restoring force characteristic is considered the similar degrading trilinear property to that of column, as shown in Fig.2, only between the bending moment and the tangential rotation angle.

Equilibrium Equation Between Incremental Stress and Strain of Member First, the equilibrium equation between the incremental stress, $\{dQ\}=\{dQ_U,\ dQ_D\}^T$, and the deformation, $\{dq\}=\{dq_U,\ dq_D\}^T$, at the ends (U and D) of member, is derived in the form of having the 4X4 flexibility matrix $[D]$.

$$\{dq\}=[D]\{dQ\},\quad \{dq\}=\{d\theta_U,\ d\omega_U,\ d\theta_D,\ d\omega_D\}^T \tag{1}$$

In Eq(1), there are 9 kind of the flexibility matrix corresponding the both ends of a member. As the typical example, the derivation of Eq(1) in case where the both ends are in the state of yield is indicated hereinafter. The incremental deformation at the ends $\{dq\}$ is expressed using the incremental elastic deformation $\{dq^e\}$, the incremental crack plastic deformation $\{dq^c\}$ and the incremental yield plastic deformation $\{dq^y\}$.

$$\{dq\}=\{dq^e\}+\{dq^c\}+\{dq^y\} \tag{2}$$

According to the plastic nomality flow rule by v. Mises (Ref.2), $\{dq^c\}$ and $\{dq^y\}$ are expressed in the following equation.

$$\{dq^c\}=[F]\{d\lambda^c\},\qquad \{dq^y\}=[H]\{d\lambda^y\} \tag{3}$$

where $[F]$ and $[H]$ are matrices which are expressing the outward normal vectors at the stress point ${}_nP$ on the crack surface ${}_nf=0$ and the yield surface ${}_nh=0$, respectively. The elements of $\{d\lambda^c\}$ and $\{d\lambda^y\}$ are real plus numbers $d\lambda_U^c$, $d\lambda_D^c$ and $d\lambda_U^y$, $d\lambda_D^y$, respectively. The incremental end stressed by $\{dq^c\}$ and $\{dq^y\}$ are assumed followingly.

$$\{dQ^c\}=[\tilde{K}^c]\{dq^c\},\qquad \{dQ^y\}=[\tilde{K}^y]\{dq^y\} \tag{4}$$

where, $[\tilde{K}^c]$ and $[\tilde{K}^y]$ are the stiffness matrices which express the strain hardening after the crack and the yield, respectively. The total incremental end stress $\{dQ\}$ is assumed as follows

$$\{dQ\}=\{dQ^e\}+\{dQ^c\}+\{dQ^y\} \tag{5}$$

where $\{dQ^e\}$is the incremental end stress by $\{dq^e\}$.
From both the normality between $\{dQ^e+dQ^y\}$ and the normal line at the stress point ${}_nP$ on the crack surface ${}_nf=0$, and the normality between $\{dQ^e+dQ^c\}$ and the normal line at the stress point ${}_nP$ on the yield surface ${}_nh=0$, the following quation can be derived using Eq.(3)-(5).

$$[F](\{dQ\}-[\tilde{K}^c][F]\{d\lambda^c\})=\{O\} \tag{6}$$

$$[H](\{dQ\}-[\tilde{K}^y][H]\{d\lambda^y\})=\{O\} \tag{7}$$

where {O} expressed null vector.
Eq.(6) and (7) are solved as to the constants, $d\lambda_U^c$, $d\lambda_D^c$ and $d\lambda_U^y$, $d\lambda_D^y$,

respectively. Substituting these constants into Eq.(3), $\{dq^c\}$ and $\{dq^y\}$ can be obtained. Next, substituting $\{dq^c\}$ and $\{dq^y\}$ into Eq.(2), the incremental equilibrium equation in the yield state of member corresponding Eq.(1) can be obtained.

The final stiffness matrix of a member in the local coordinate system can be obtained by introducing shearing deformation in Eq.(1).

ANALYSES OF STRUCTURAL TESTS OF COLUMNS WITH CORE REBARS IN THEIR CENTER

Outline of Structural Tests Analytical objects are the two columns which are laterally loaded under a fluctuating large axial force (Ref.3). Two specimens representing exterior columns on the 2nd story of a 30 story RC building are 1:2.6 - scale columns which have 16 longitudinal rebars with 8 core rebars in their centers and incorporate both spiral and square hoop, as shown in Fig.4.

Two specimens, No.1 and 2 after the axial force $N_L=84_{tf}$ corresponding to the design permanent axial force, are subjected to both horizontal and vertical earthquake forces (Q and N_L+N_K) whose ratio Q/N_K is determined to be 1/18 based on the design static analytical results of the 30 story building against lateral earthquake loads. No.1 specimen which is supposed to be the exterior column in the tension side is loaded until final horizontal distortion under the tension, while No.2 which is supposed to be the exterior column in the compression side under compression.

Analytical Model It is assumed that the screened part shown in Fig.4 is subjected to the cyclic reversed loadings which consist of the anti-symmetric distributed moment and the axial force.

The constants, which prescribe the stiffness reduction ratio α^M , α^N shown in Fig.2 and 3, are assumed followingly. Where α^{tM} , which is the stiffness reduction ratio in the M-Θ skelton curve under constant axial force N=No, is assumed so that the M-Θ gradient between the origin and the yield point may be the one which is calculated based on Ref.4. α^{cN} which is the compression stiffness reduction ratio in the uniaxial N-ω skelton curve is assumed so that the yield compressive axial strain may be 0.002, while α^{tN} which is the tension stiffness reduction ratio is assumed so that the yield tensile axial strain may be the yield strain of the reinforcing bar. The bending and axial stiffness reduction ratio p^M and p^N in the yield state is assumed 0.02 and 0.005, respectively.

The Analytical Results of No.1 Specimen The tested and analyzed Q-δ curve of Nq 1 specimen is shown in Fig.5 and 6, respectively. In the region where the sign of Q is plus, the analyzed curve is almost quadinear in the four states of the elastic, the crack under fluctuating axial force, the crack under constant axial force and the yield. Although the gradient in the crack state under constant axial force in the analyzed Q-δ curve is steeper than that in the tested, the analyzed almost approximates the tested.

The Analytical Results of No.2 Specimen The tested and analyzed Q-δ curve is shown in Fig.7 and Fig.8 respectively. The analyzed shows a almost good approximation. But the tested indicates the strength reduction on an account of the large compression. Otherwise, since the strength reduction effect is not considered in the analyzed, the analyzed cannot express the negative gradient caused due to the large compression in the tested.

EARTHQUAKE RESPONSE ANALYSIS OF A 30 STORY RC FRAME

Analytical Object of a RC Frame and Analytical Condition Analytical object of a RC frame is a typical one of the frames which compose of a 30 story RC Building

in the city of Kawasaki, as shown in Fig.9. Structural characteristic of this building is to adopt the high strength concrete up to the design strength of 420kgf/cm^2 and the columns with core rebars in their centers. With regard to the yielding mechanism of the framing structure, it is designed that the strength of column is 1.25 times more than that of beam in order that bending yieldings of beams precede those of columns except the columns of the top and 1st story. The crack surface, the yield surface and the nonlinear characteristics are assumed by the same way as in the aforementioned simulation analysis of the structural test.

The input adopted earthquake motion is EL CENTRO 1940 NS whose maximum velocity of 75 cm/sec. The input duration time and the time interval is 12 sec. and 0.005 sec., respectively. Internal viscous damping is used assuming 3% damping factor for the 1st vibration period of 1.64 sec.

Analytical Results Occurrence of cracks and yields after the end of earthquake motion is shown in Fig.10.

The max. response story drift angle and the max. ductility factor at the beam ends is shown in Fig.11 and 12, respectively. The ductility factor 2.5 at the beam end on the 15th floor is the largest and it results that the story drift angle 1/100 of the 15th story is the largest of all. The response hysteresis curve between the story shear force (Q) and story drift(δ) at the 15th story is shown in Fig.13. The M-θ hysteresis curve at the 5th span beam at the right end on the 15th floor where the largest plastic deformation develops is shown in Fig.14.

The M-θ response curve at the left side exterior column and the center column is shown in Fig.15. The M-θ curve of the exterior column presents the complex behavior especially under the tension due to the fluctuation of the axial force since the M-N interuction effect in the plastic range become larger on the exterior column than on the interior one.

The motion of the M-N response force points at the bottoms of the left side column and the center column are shown in Fig.16 along with the transfer and expantion of the crack and yield surfaces between 4 and 6 sec. when its severest response is presented. In the exterior column, the increase and decrease of N is larger than those of M in the yield state, and the absolute value of M decrease a little especially under the tension. And it results that the minus gradients can be caused in the M-θ curve.

CONCLUSION

From the results of the studies, the adequacy and usefulness of this analytical method are verified. It is, therefore, confirmed that the earthquake resistant design of the highrise RC building is upgraded by using this method.

REFERENCES

1. Muto, K., et al., "Earthquake Resistant Design of a 20 Story Reinforced Concrete Building", Proceeding of the 5th World Conference on Earthquake Engineering, Vol.2, (1973)
2. Mises, Von R., "Mechanik der Plastishen Formandering der Kristallen", Z.angew. Math. Mech., 8, (1928)
3. Bessho, S., et al., "Earthquake Resistant Design of a 30 Story Reinforced Concrete Building, Part IV Lateral Loading Tests of Exterior Columns" Proceeding of Annual Conference of Archtectural Institute of Japan, (1985)
4 Architectural Institute of Japan, "AIJ Standard for Structural Calculation of Reinforced Concrete Structures"

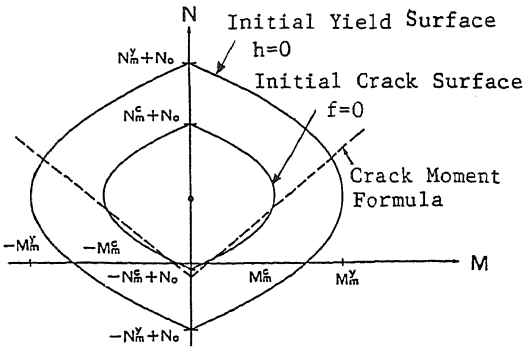

Fig.1 Initial Crack and Yield Surfaces

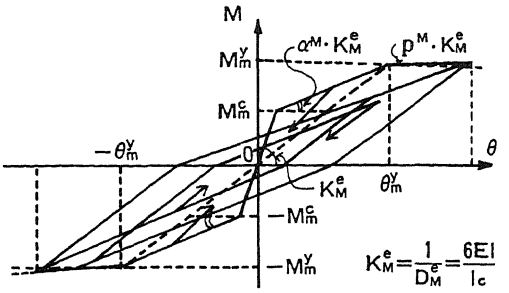

Fig.2 Assumed Uniaxial M-Θ Hysteresis Loop

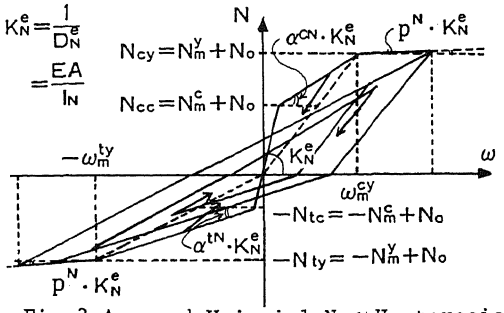

Fig.3 Assumed Uniaxial N-ω Hysteresis Loop

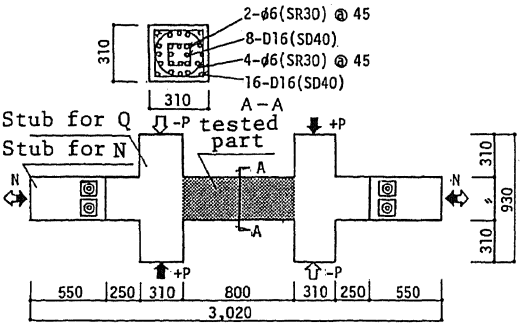

Fig.4 Structural Test Specimen of Column with Core Rebars

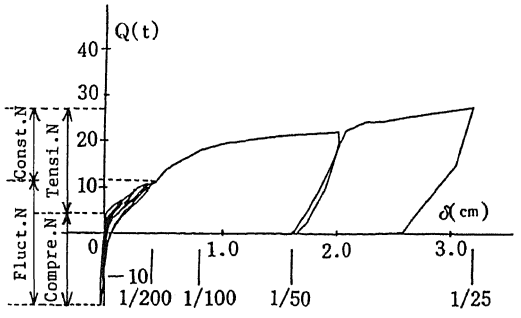

Fig.5 Tested Q-δ Curve of No.1 Specimen

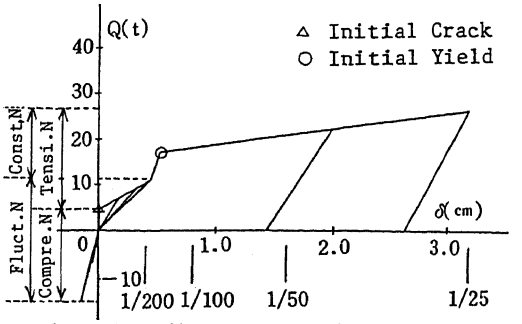

Fig.6 Analyzed Q-δ Curve of No.1 Specimen

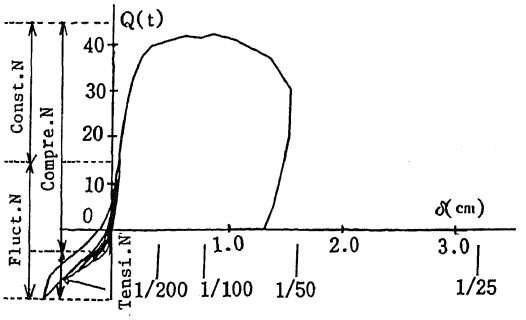

Fig.7 Tested Q-δ Curve of No.2 Specimen

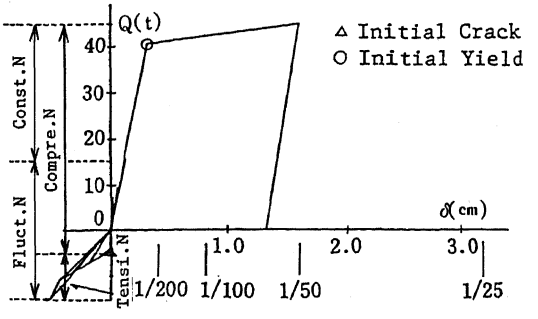

Fig.8 Analyzed Q-δ Curve of No.2 Specimen

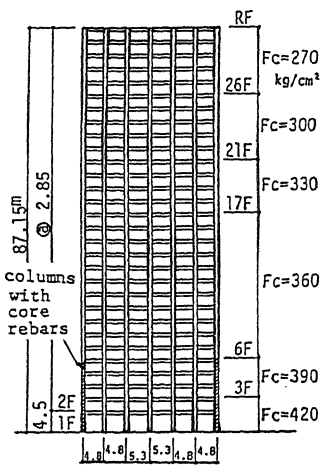

Fig.9 Analytical Object of a RC Frame

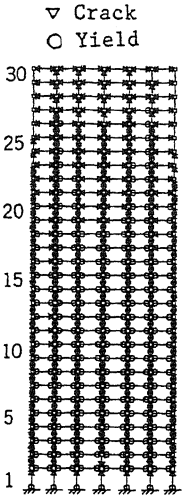

Fig.10 Occurrence of Crack and Yield after EQ.

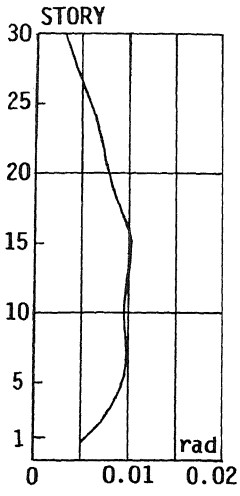

Fig.11 Max. Story Drift Angle

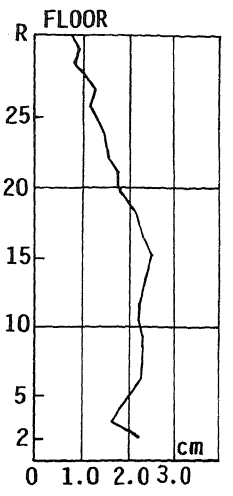

Fig.12 Max. Ductility factor of Beam End

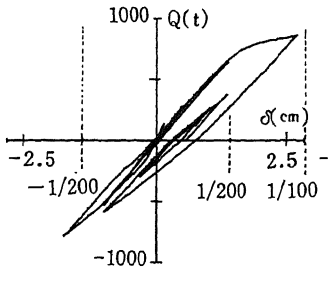

Fig.13 Q-δ Hysteresis Loop at the 15th Story

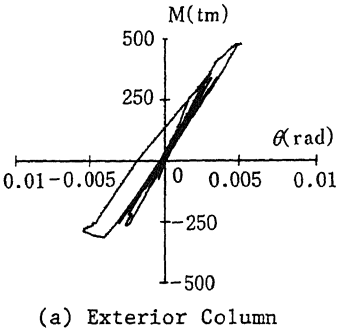

(a) Exterior Column

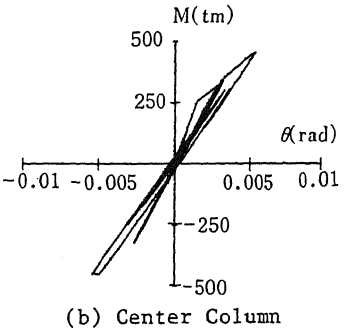

(b) Center Column

Fig.15 M-θ Hysteresis Loop at bottom of the 1st Story Column

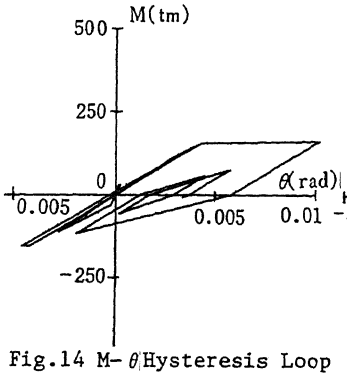

Fig.14 M-θ Hysteresis Loop at Beam End on the 15th Floor

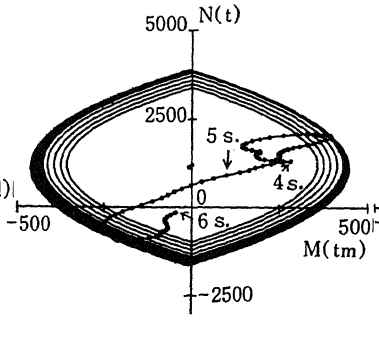

(a) Exterior Column

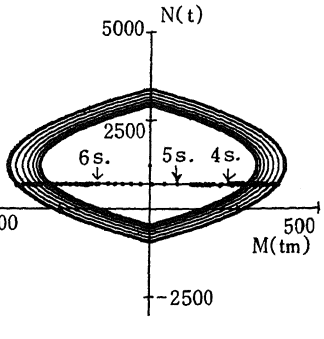

(b) Center Column

Fig.16 MN Response Orbit and Surfaces at bottom of the 1st Story Column